

Template synthesis of ordered arrays of mesoporous titania spheres†

Jianfeng Chen,^{ab} Zhongjiong Hua,^a Yushan Yan,^c Anvar A. Zakhidov,^d Ray H. Baughman^d
and Lianbin Xu^{*ac}

Received (in Cambridge, UK) 31st July 2009, Accepted 10th December 2009

First published as an Advance Article on the web 13th January 2010

DOI: 10.1039/b915706a

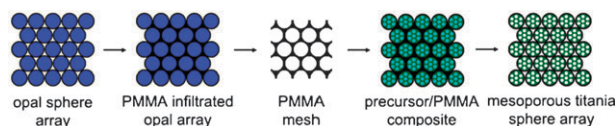
Three-dimensionally ordered arrays of submicron-sized mesoporous titania spheres with high surface area and high crystallinity have been prepared through triblock copolymer templating within the confinement of polymer inverse opals.

Ordered mesoporous titania (TiO₂) materials with a crystalline framework, high specific surface area and tailored pore structure are of great interest for applications in a variety of areas, including photocatalysis, photovoltaic cells, lithium batteries, and gas sensing.¹ Various synthetic strategies using different structure-directing soft templates, such as block copolymers, anionic surfactants, cationic surfactants, and primary amines have been developed to prepare crystalline TiO₂ with well-defined mesopores.² Mesoporous TiO₂ materials are typically produced as bulk powders and films. Recently, mesoporous TiO₂ spheres in the micron- and submicron-size range have attracted much attention owing to their broad applications in catalysis, energy conversion, and biotechnology.³ The organization of submicron-sized mesoporous TiO₂ spheres into three-dimensionally (3D) ordered close-packed arrays would be important for specific applications. For example, 3D ordered arrays of mesoporous TiO₂ spheres, which act as photonic crystals,⁴ and contain hierarchical macropores (the voids between the close-packed spheres) and mesopores, would be desirable to improve the photocatalytic activity due to the high specific surface area, enhanced photoabsorption efficiency, and efficient molecule diffusion.^{1a,5} They could also be used as 3D electrode materials for lithium batteries.⁶ However, it is still challenging to fabricate 3D ordered TiO₂ sphere arrays through traditional colloidal crystal self-assembly technique due to the difficulty in obtaining highly uniform and monodisperse mesoporous TiO₂ spheres. The mesoporous TiO₂ particles previously prepared are generally polydisperse and not spherical in some cases.^{3a-d} Tang *et al.* designed a two-step nanocasting route to prepare monodisperse mesoporous TiO₂ spheres employing mesoporous

silica spheres and carbon spheres as the first template and second template, respectively.^{3e} However, the high temperature used for the formation and removal of the mesoporous carbon sphere template tended to deteriorate the mesostructural ordering, resulting in disordered mesopores of TiO₂ spheres; also the packing of mesoporous TiO₂ spheres into regular arrays was not demonstrated. In this work, we report the fabrication of 3D ordered arrays of TiO₂ spheres with well-defined mesopores through a combination of two-step micromolding (hard-templating) and triblock-copolymer-templating (soft-templating) approaches, removing the need for the production of monodisperse mesoporous TiO₂ spheres.

By the use of opal (ordered close-packed face-centered cubic (fcc) lattice of silica or latex spheres) as a template, inverse opal (macroporous mesh) can be readily fabricated by established methods.⁷ Then the mesh can be further used as a mold to synthesize a variety of materials composed of ordered sphere arrays.⁸ We have employed this two-step micromolding method to fabricate highly ordered metal sphere arrays.^{8a,b} Through the incorporation of a surfactant template as a mesopore-structure-directing agent, ordered mesoporous silica sphere arrays have been successfully prepared by Ozin *et al.*^{8d} and Braun *et al.*^{8e} Herein, we extend this technique to fabricate 3D ordered mesoporous TiO₂ sphere arrays. To the best of our knowledge, this study demonstrates for the first time the synthesis of highly ordered arrays of mesoporous metal oxide spheres. It is known that the morphology control and confinement of mesoporous metal oxides are more difficult than that of silica due to the high reactivity of hydrolysis and condensation of metal ion precursors.^{1d,3a,f,9,10}

Scheme 1 illustrates the procedure for the fabrication of ordered mesoporous TiO₂ sphere arrays. Opal templates were prepared by the methods previously described.¹¹ The highly ordered single-crystal-like opal pieces were composed of 290 nm silica spheres. A piece of silica opal was immersed in methyl methacrylate (MMA) monomer with 1 wt% benzoyl peroxide (BPO) as an initiator. Polymerization was initially carried out at 40 °C for 10 h and then 60 °C for 12 h. The silica opal spheres were removed using a 10 wt% HF solution (24 h) to obtain a freestanding PMMA mesh (inverse opal). The PMMA mesh was used as the second-step template for the



Scheme 1 Schematic of two-step replication process for the fabrication of ordered arrays of mesoporous TiO₂ spheres.

^a Key Lab for Nanomaterials, Ministry of Education, Beijing University of Chemical Technology, Beijing, 100029, China. E-mail: lbxu99@gmail.com; Fax: +86-10-64434784; Tel: +86-10-64449241

^b Research Center of the Ministry of Education for High Gravity Engineering and Technology, Beijing University of Chemical Technology, Beijing, 100029, China

^c Department of Chemical and Environmental Engineering, University of California, Riverside, CA 92521, USA

^d The Alan G. Macdiarmid NanoTech Institute, University of Texas at Dallas, Richardson, TX 75083, USA

† Electronic supplementary information (ESI) available: Experimental details, XRD patterns for calcined samples, SEM and TEM images. See DOI: 10.1039/b915706a

formation of ordered TiO_2 spheres, and amphiphilic triblock copolymer Pluronic P123 ($\text{EO}_{20}\text{PO}_{70}\text{EO}_{20}$) acted as a structure-directing agent to make the mesopores. The titania precursor solution contained 2.84 g titanium tetraisopropoxide (TTIP), 2.4 g concentrated HCl (37 wt%), 1.16 g P123 and 3.7 g ethanol. The titania precursor solution was infiltrated into the spherical macropores of the PMMA mesh by immersing the mesh in the precursor solution for 4 h. After that, the precursor-filled PMMA mesh was removed from the solution, and then aged at room temperature for 3 days. Ordered mesoporous TiO_2 sphere arrays were obtained by heating the precursor/PMMA composite in open air to $400\text{ }^\circ\text{C}$ at $1\text{ }^\circ\text{C min}^{-1}$, followed by a 4 h soak to remove the PMMA mesh template and the triblock copolymer surfactant.

Fig. 1a shows a typical scanning electron microscopy (SEM) image of a piece of opal consisting of 3D ordered silica spheres with 290 nm diameter. The PMMA mesh (Fig. 1b) produced from the opal template exhibits a uniform porous structure that is the inverse of the original opal. Since the macropores in PMMA mesh are interconnected, the PMMA mesh allows the titania precursor solution to diffuse through the mesh and fill the pores in the PMMA mesh. After calcination to remove both the PMMA mesh template and the P123 surfactant template, ordered mesoporous TiO_2 sphere arrays were formed (Fig. 1c). Fig. 1d reveals an SEM image of predominately the (111) orientation of mesoporous TiO_2 sphere arrays. Through this two-step replication procedure, as-prepared mesoporous TiO_2 still keeps the spherical shape and ordered close-packed fcc structure as in the initial silica opal, but the diameter of the mesoporous TiO_2 spheres is observed to be *ca.* 165 nm, $\sim 40\%$ smaller than the original silica sphere diameter. This volume shrinkage is due to the condensation of the titania precursor during calcination.¹²

Transmission electron microscopy (TEM) and high-resolution TEM (HR-TEM) were used to examine the mesoporous

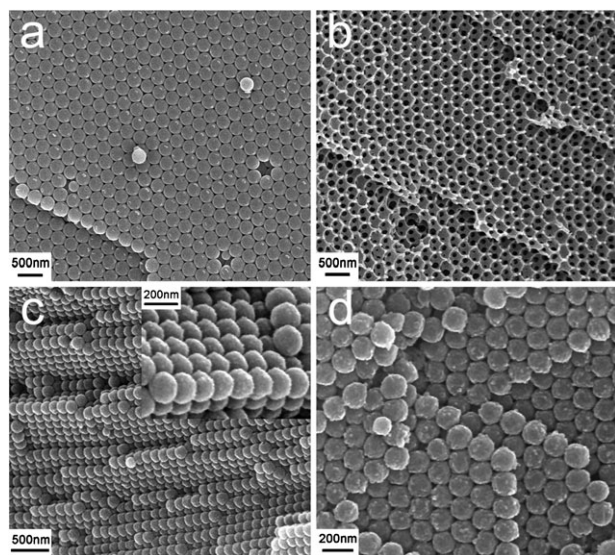


Fig. 1 SEM images of (a) an opal sample consisting of 290 nm diameter silica spheres, (b) a PMMA mesh after the removal of the silica spheres, (c) a cross-section of mesoporous TiO_2 sphere arrays, inset: at a higher magnification, (d) mesoporous TiO_2 sphere arrays with (111) orientation.

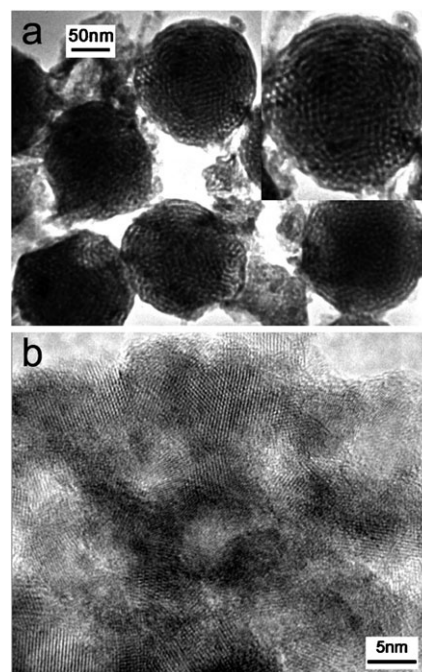


Fig. 2 (a) TEM image of mesoporous TiO_2 spheres, inset: higher magnification image of one of the mesoporous TiO_2 spheres. (b) HR-TEM image of mesoporous TiO_2 spheres.

structure and crystallization of the TiO_2 spheres. Fig. 2a shows a typical TEM image of these TiO_2 spheres. One of the spheres has been enlarged in the inset of Fig. 2a. The ordered mesoporous structure can be observed in the TEM images. The corresponding HR-TEM image (Fig. 2b) reveals that a porous mesostructure and high crystallinity coexist in the mesoporous TiO_2 sample. The mesopore size is in the range of 3–5 nm, and the TiO_2 nanocrystallites have diameter of 7–10 nm. The lattice fringes of 0.35 nm observed in the mesopore walls correspond to the d-spacing between adjacent (101) crystallographic planes of anatase TiO_2 phase.

X-Ray diffraction (XRD) was employed to further investigate the crystalline phase and particle size of the mesoporous TiO_2 sphere arrays. The XRD pattern (Cu-K α radiation, $\lambda = 1.5418\text{ \AA}$) (Fig. 3) exhibits diffraction peaks at 2θ of 25.4° , 37.8° , 48.1° , 54.0° , 55.2° , and 62.8° , which can be readily indexed to the anatase phase of TiO_2 (JCPDS card, No. 21-1272). The broadening of the diffraction peaks suggests that the walls of the mesoporous TiO_2 spheres consist of nanocrystalline anatase, consistent with the HR-TEM investigation. The crystalline size estimated using the Scherrer equation from the full width at half maximum (FWHM) of the (101) peak ($2\theta = 25.4^\circ$) is $\sim 8.5\text{ nm}$, which is in agreement with the HR-TEM observation.

The nitrogen adsorption/desorption isotherm of as-prepared mesoporous TiO_2 spheres is shown in Fig. 4. The isotherm can be classified as type IV, typical for mesoporous materials according to the IUPAC nomenclature.¹³ Two hysteresis loops appear in the isotherm. The hysteresis loop at low relative pressure between 0.40 and 0.82, is of type H2, and can be ascribed to capillary condensation in mesopores generated by the surfactant P123. The other loop at high relative pressure between 0.86 and 1.0 has a type H3 shape, which may

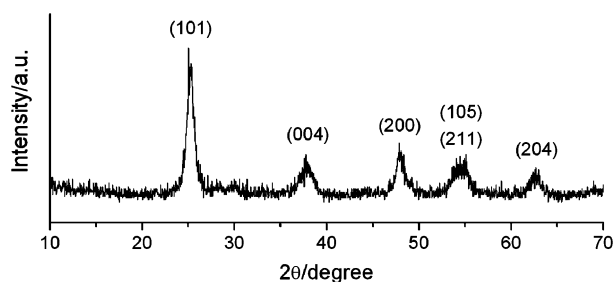


Fig. 3 XRD pattern of mesoporous TiO₂ sphere arrays.

represent interparticle pores within the sample.¹⁴ The Brunauer–Emmett–Teller (BET) surface area and pore volume of the mesoporous TiO₂ spheres are 145 m² g⁻¹ and 0.246 cm³ g⁻¹, respectively. The inset in Fig. 4 shows the pore size distribution calculated by the Barrett–Joyner–Halenda (BJH) method using the desorption isotherm. The average pore diameter of the mesoporous TiO₂ spheres is 3.6 nm. In addition, the mesopore size distribution is in the range of 2–6 nm, and such a narrow distribution implies substantial homogeneity of the mesopores for the TiO₂ spheres. The BJH pore size distribution results agree well with the TEM and HR-TEM characterizations.

In summary, 3D ordered arrays of mesoporous TiO₂ spheres have been successfully fabricated by using PMMA inverse opal and triblock copolymer Pluronic P123 as templates. The prepared TiO₂ spheres exhibit a well-defined mesoporous structure and are composed of nanocrystalline anatase titania. Due to their unique porous structure and three-dimensional periodicity, the ordered mesoporous TiO₂ sphere arrays may find numerous applications, for example, in photocatalysis, photonics, solar energy conversion, and rechargeable lithium batteries. It is expected that the present method can be easily extended to the similar ordered mesoporous spherical structures of other metal oxide materials, such as Al₂O₃, and ZrO₂.

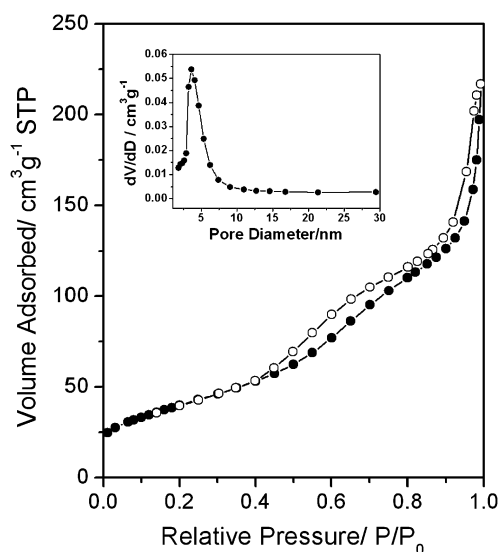


Fig. 4 Nitrogen adsorption/desorption isotherm and pore size distribution curve (inset) for mesoporous TiO₂ sphere arrays.

The authors gratefully acknowledge financial support from the National Science Foundation of China (20971012 and 20821004), National 973 Program of China (2009CB219903), Robert A. Welch Foundation (AT-0029), and US Air Force Office of Scientific Research (FA-9550-05-1-09-09).

Notes and references

- (a) C. Aprile, A. Corma and H. Garcia, *Phys. Chem. Chem. Phys.*, 2008, **10**, 769; (b) M. A. Carreon, S. Y. Choi, M. Mamak, N. Chopra and G. A. Ozin, *J. Mater. Chem.*, 2007, **17**, 82; (c) M. Zukulova, A. Zukul, L. Kavan, M. K. Nazeeruddin, P. Liska and M. Gratzel, *Nano Lett.*, 2005, **5**, 1789; (d) K. X. Wang, M. D. Wei, M. A. Morris, H. S. Zhou and J. D. Holmes, *Adv. Mater.*, 2007, **19**, 3016; (e) G. S. Devi, T. Hyodo, Y. Shimizu and M. Egashira, *Sens. Actuators, B*, 2002, **87**, 122; (f) X. B. Chen and S. S. Mao, *Chem. Rev.*, 2007, **107**, 2891.
- (a) P. D. Yang, D. Y. Zhao, D. I. Margolese, B. F. Chmelka and G. D. Stucky, *Nature*, 1998, **396**, 152; (b) E. L. Crepaldi, G. J. A. A. Soler-Illia, D. Grosso, F. Cagnol, F. Ribot and C. Sanchez, *J. Am. Chem. Soc.*, 2003, **125**, 9770; (c) H. M. Luo, C. Wang and Y. S. Yan, *Chem. Mater.*, 2003, **15**, 3841; (d) D. M. Antonelli and J. Y. Ying, *Angew. Chem., Int. Ed. Engl.*, 1995, **34**, 2014; (e) V. Luca, J. N. Watson, M. Ruschena and R. B. Knott, *Chem. Mater.*, 2006, **18**, 1156; (f) H. Shibata, T. Ogura, T. Mukai, T. Ohkubo, H. Sakai and M. Abe, *J. Am. Chem. Soc.*, 2005, **127**, 16396; (g) G. J. A. A. Soler-Illia, A. Louis and C. Sanchez, *Chem. Mater.*, 2002, **14**, 750; (h) T. Sreethawong, Y. Suzuki and S. Yoshikawa, *Catal. Commun.*, 2005, **6**, 119.
- (a) C. K. Tsung, J. Fan, N. F. Zheng, Q. H. Shi, A. J. Forman, J. F. Wang and G. D. Stucky, *Angew. Chem., Int. Ed.*, 2008, **47**, 8682; (b) D. Grosso, G. J. A. A. Soler-Illia, E. L. Crepaldi, B. Charleux and C. Sanchez, *Adv. Funct. Mater.*, 2003, **13**, 37; (c) Y. X. Zhang, G. H. Li, Y. C. Wu, Y. Y. Luo and L. D. Zhang, *J. Phys. Chem. B*, 2005, **109**, 5478; (d) Y. J. Kim, M. H. Lee, H. J. Kim, G. Lim, Y. S. Choi, N. G. Park, K. Kim and W. I. Lee, *Adv. Mater.*, 2009, **21**, 3668; (e) A. G. Dong, N. Ren, Y. Tang, Y. J. Wang, Y. H. Zhang, W. M. Hua and Z. Gao, *J. Am. Chem. Soc.*, 2003, **125**, 4976; (f) H. F. Yang, Y. Yan and D. Y. Zhao, *J. Ind. Eng. Chem.*, 2004, **10**, 1146.
- X. C. Jiang, T. Herricks and Y. N. Xia, *Adv. Mater.*, 2003, **15**, 1205.
- X. C. Wang, J. C. Yu, C. M. Ho, Y. D. Hou and X. Z. Fu, *Langmuir*, 2005, **21**, 2552.
- J. W. Long, B. Dunn, D. R. Rolison and H. S. White, *Chem. Rev.*, 2004, **104**, 4463.
- A. Stein and R. C. Schroden, *Curr. Opin. Solid State Mater. Sci.*, 2001, **5**, 553.
- (a) L. B. Xu, L. D. Tung, L. Spinu, A. A. Zakhidov, R. H. Baughman and J. B. Wiley, *Adv. Mater.*, 2003, **15**, 1562; (b) L. B. Xu, W. L. Zhou, M. E. Kozlov, I. I. Khayrullin, I. Udod, A. A. Zakhidov, R. H. Baughman and J. B. Wiley, *J. Am. Chem. Soc.*, 2001, **123**, 763; (c) P. Jiang, J. F. Bertone and V. L. Colvin, *Science*, 2001, **291**, 453; (d) S. M. Yang, N. Coombs and G. A. Ozin, *Adv. Mater.*, 2000, **12**, 1940; (e) W. S. Chae and P. V. Braun, *Chem. Mater.*, 2007, **19**, 5593; (f) W. C. Yoo, S. Kumar, Z. Y. Wang, N. S. Ergang, W. Fan, G. N. Karanikolos, A. V. McCormick, R. L. Penn, M. Tsapatsis and A. Stein, *Angew. Chem., Int. Ed.*, 2008, **47**, 9096.
- S. Y. Choi, M. Mamak, N. Coombs, N. Chopra and G. A. Ozin, *Adv. Funct. Mater.*, 2004, **14**, 335.
- W. S. Chae, S. W. Lee and Y. R. Kim, *Chem. Mater.*, 2005, **17**, 3072.
- A. A. Zakhidov, R. H. Baughman, Z. Iqbal, C. X. Cui, I. Khayrullin, S. O. Dantas, J. Marti and V. G. Ralchenko, *Science*, 1998, **282**, 897.
- K. M. Coakley, Y. X. Liu, M. D. McGehee, K. L. Frindell and G. D. Stucky, *Adv. Funct. Mater.*, 2003, **13**, 301.
- K. S. W. Sing, D. H. Everett, R. A. W. Haul, L. Moscou, R. A. Pierotti, J. Rouquerol and T. Siemieniewska, *Pure Appl. Chem.*, 1985, **57**, 603.
- (a) Y. Han and J. Y. Ying, *Angew. Chem., Int. Ed.*, 2005, **44**, 288; (b) Z. Y. Wang and A. Stein, *Chem. Mater.*, 2008, **20**, 1029.